# A theoretical study of electron–hole pair formation due to the collision of an atom with a solid surface

Y. Zeiri
*Department of Physics, Nuclear Research Center-Negev, P.O. box 9001 Beer-Sheva, Israel*

R. Kosloff
*Department of Physical Chemistry and The Fritz Haber Research Center for Molecular Dynamics, The Hebrew University, Jerusalem 91904, Israel*

(Received 18 June 1990; accepted 16 July 1990)

Electronic excitation in a semiconductor induced by the collision of energetic atoms with the solid surface is investigated theoretically. The modeling has been performed for a one-dimensional independent-electron system where the solid is described by a chain of 10–20 atoms. The time evolution of the nuclei (i.e., colliding atom and chain atoms) has been described by classical mechanics while quantum mechanical description has been used for the electronic dynamics. The two systems (i.e., the atoms and the electron) were coupled to each other and the equations of motion were solved self-consistently. Energy dissipation from the chain to the rest of the solid was included via the GLE approach. This study establishes the relationship between the probability of electron–hole formation and various parameters of the system such as collider translational energy, magnitude of the band gap, and existence of impurities in the solid. In addition, two excitation mechanisms were examined, electronic excitation due to a direct coupling between the electron and the colliding atom and an indirect mechanism due to electron–phonon coupling.

## I. INTRODUCTION

The scattering of hyperthermal molecular and atomic beams from solid surfaces is a phenomenon of considerable interest. Recently, a number of detailed studies of the dynamics of various physical and chemical phenomena which incorporate hyperthermal particle–surface collisions were performed. These include: (A) collision induced desorption,[1,2] (B) energy transfer during particle–surface collision,[3] (C) dissociation and adsorption of molecules induced by high kinetic energy impact on solid surfaces,[3–7] and (D) surface induced ionization.[8] In addition, a number of research teams have studied the possibility of electronic excitation during particle scattering at the surfaces and the role of such processes as an additional channel for energy dissipation.[9–11] Most of these studies are related to the collision of a particle with a metallic surface. For such systems, where the conduction band is partially filled, one would expect that a significant fraction of the collision energy may be channeled into the excitation of the metal electrons. The situation is different for semiconductor or insulator surfaces for which very small electronic excitation is expected if the collision energy is smaller than the band gap. Recently, Amirav and Cardillo and Weiss *et al.* have reported the results of an experiment in which electron–hole pairs were created by the impact of an atomic beam on an InP(100) surface.[12] The analysis of these results have shown a very high yield of electron–hole pair formation (i.e., about 30% for excitation by an energetic Xe beam). The estimation of this high excitation probability was based on an approximate expression which converted the measured currents to a density of excited electrons.

The problem addressed in this work is to understand the basic mechanisms which leads to the creation of electron–hole pairs. The two main possible mechanisms are: (1) direct coupling of the projectile to the electronic degrees of freedom in the solid and (2) an indirect process in which electron–phonon coupling is the main source for the excitation. The first mechanism has been studied for the case in which various atoms impact a metallic surface with collision energy in the range of 1.0–100.0 eV.[9] It has been found that a significant fraction of the collision energy was transferred to the metal electrons. To the best of our knowledge, indirect mechanisms have not been examined so far in the context of electronic excitation due to the impact of an energetic particle.

The goal of the present work is to formulate a theoretical model by which the excitation of electron–hole pairs in a semiconductor by the impact of a gas particle can be studied. In particular, this study focuses on the comparison between the two possible mechanisms and the evaluation of their relative importance in gas–solid interactions. In addition, the relation between excitation probability and various parameters of the system, such as projectile energy, magnitude of the band gap, existence of impurities and defects, were examined. In the next section, the theoretical model used in the present study will be described. Section III describes and discussion of the results. The last section is devoted to a short summary.

## II. THEORETICAL FRAMEWORK

The goal of this section is to outline a consistent procedure for modeling the electronic excitation. The physical

 0021-9606/90/216890-10$03.00 

system under investigation is very demanding. The main problem relates to its multiple bodied aspect so that a full quantum mechanical description of all degrees of freedom is beyond current computational capabilities. A practical modeling of the processes involved require a hierarchial procedure in which only the relevant degrees of freedom are treated in a full quantum mechanical fashion. Other degrees of freedom are described by a classical or semiclassical approximation. The correct many-body solution is formally solved by the Liouville–von Neumann equation for the density operator:

$$\frac{\partial\hat{\rho}}{\partial t}=L\hat{\rho}, \tag{2.1}$$

where the Liouville operator can be separated into individual contributions:

$$L=L_g+L_s+L_b+L_e+L_{gs}+L_{es}+L_{eg}+L_{sb}, \tag{2.2}$$

where the subscript $g$ indicates the colliding atom, $s$ the solid, $b$ the thermal bath, and $e$ the electrons in the solid. Higher correlations such as three-body terms are omitted. The main approximation is to use a mean field approach which separates the full density operator into a tensor product of the density operators for nuclear and electronic motion:

$$\hat{\rho}\approx\hat{\rho}_{gsb}\otimes\hat{\rho}_e. \tag{2.3}$$

This separation replaces the full multiple bodied correlated motion with a mean field interaction:

$$\frac{\partial\hat{\rho}_{gsb}}{\partial t}=(L_g+L_s+L_b+L_{gs}+L_{sb})\hat{\rho}_{gsb}+[\mathrm{tr}_e(L_{ge}\hat{\rho}_e+L_{se}\hat{\rho}_e)]\hat{\rho}_{gsb}, \tag{2.4a}$$

$$\frac{\partial\hat{\rho}_e}{\partial t}=L_e\hat{\rho}_e+[\mathrm{tr}_{gsb}(L_{ge}\hat{\rho}_{gsb}+L_{se}\hat{\rho}_{gsb})]\hat{\rho}_e. \tag{2.4b}$$

Once a partition of the density has been made, each of the two parts can be treated in different fashion. In this paper the nuclear motion is described classically and the electrons are described quantumly. The thermal motion of the solid which is not included explicitly in the calculation, is introduced through a generalized Langevin approach.[1(a),13]

The next approximation is to omit electron electron interactions. This reduces the electronic description to a single electron density function. Approximating the initial state by the ground initial state (zero temperature) in the mean field approximation reduces Eq. (2.4b) to a Schrödinger-type equation:

$$i\hbar\frac{\partial\psi_e}{\partial t}=\{\hat{\mathbf{H}}_e+\hat{\mathbf{V}}_{es}(\mathbf{R}_s)+\hat{\mathbf{V}}_{eg}(\mathbf{R}_g)\}\psi_e, \tag{2.5a}$$

where

$$\hat{\rho}_e=|\psi_e\rangle\langle\psi_e|$$

and $\hat{\mathbf{H}}_e$ is the electronic kinetic energy, $\hat{\mathbf{V}}_{es}(\mathbf{R}_s)$ is the electron solid interaction potential where $\mathbf{R}_s$ are the solid nuclear coordinates. $\hat{\mathbf{V}}_{eg}(\mathbf{R}_g)$ is the electron gas particle interaction potential where $\mathbf{R}_g$ represents the gas atom position vector. The effective potentials in Eq. (2.5a) assume a semiclassical approximation in which the averaged potential over the nuclear wave function can be replaced by the potential of the mean position. Similarly, Eq. (2.4a) is replaced by Hamiltons equations for the mean position and momentum:

$$\frac{\partial\mathbf{R}}{\partial t}=\left\langle\frac{\partial\mathbf{H}}{\partial\mathbf{P}_R}\right\rangle_e, \tag{2.5b}$$

$$\frac{\partial\mathbf{P}_R}{\partial t}=-\left\langle\frac{\partial\mathbf{H}}{\partial\mathbf{R}}\right\rangle_e,$$

where $\mathbf{H}$ is the averaged classical Hamiltonian function and $\langle\ \rangle_e$ represents an average over the electronic degrees of freedom. A generalized Langevin equation (GLE) approach[1(a),13] has been used to describe the influence of the heat bath. Explicitly the electronic part exerts a force on the solid nuclei which is calculated by the matrix element:

$$F_{ei}=\langle\psi_e|\frac{\partial\mathbf{V}_{ei}(r_i-r_e)}{\partial r_i}|\psi_e\rangle;\quad i=s,g. \tag{2.6}$$

For the electron solid nuclei interaction a screened Coulomb potential has been used:

$$\hat{\mathbf{V}}_{es}(\mathbf{R}_s)=\sum_{i=0}^{N}\mathbf{V}_{ei}(r_i), \tag{2.7}$$

where

$$\hat{\mathbf{V}}_{ei}(r_i)=\frac{Z_i}{[(r_e-r_i)^2+\alpha^2]^{1/2}}, \tag{2.8}$$

$N$ is the number of solid atoms, $Z_i$ is the average nuclear charge of atom $i$, $r_e$ the electron coordinate, $r_i$ is the $i$th nuclear coordinate, and $\alpha$ is the screening parameter. The total electron solid potential is the sum of the individual contributions. The form of the interaction potential between the gas atom and the solid chain as well as the interaction between the electron and the gas atom will be discussed in Sec. III.

The self-consistent formalism described in this section resembles the formulation used by Selloni *et al.*[14] to treat an electron in molten salt and also the description of an excess electron in water and ammonia clusters[15] and in bulk.[16]

### A. Initial state

The simulation is initiated by starting with the gas atom outside the interaction region, establishing a self-consistent initial state for the solid. The following procedure was used: First the ground state of the electronic part, with the equilibrium positions of the solid atoms, was found. The procedure used was the relaxation method in which an initial guess of the ground state is propagated by the Schrödinger equation in imaginary time. The propagation was stopped when the change in energy per time step was less than $10^{-9}$. The propagation in imaginary time was carried out using a Chebychev expansion of the evolution equation:

$$e^{-\hat{\mathbf{H}}t}\psi(0)\approx\sum_{n=0}^{N}a_n(\Delta E\cdot t/2)T_n(\mathbf{H})\psi(0), \tag{2.9}$$

where $a_n(\alpha)=I_n(\alpha)$ where $I$ represents the Bessel functions of the first kind, and $T_n$ are the Chebychev polynomials which are calculated by their recursion relation. $\Delta E$ is the energy range represented on the grid. Details of the method can be found elsewhere.[17] Once the ground electronic state was found the electron surface nuclei forces are calculated

by using relation (2.7) which is then used to find a new equilibrium state of the solid. This is done by bleeding the kinetic energy of the solid until a new equilibrium is established. The procedure is continued until a combined cold initial state is reached. The initial position of the incoming particle is chosen outside the interaction region. The initial momentum is chosen to correspond to the initial gas kinetic energy.

### B. Propagating the system

First the equations of motion (2.5), combined with the classical part, are propagated self-consistently. The electronic wave function is represented on a spatial grid by using the Fourier method[18] to calculate the kinetic energy operator. The electronic equations of motion are then propagated by using a Chebychev expansion of the evolution equation. This propagation method has extremely high accuracy which allows the detection of extremely small excitations.[18] The nuclei equations of motion are next propagated using a standard integrator synchronized with the electronic propagation. The typical grid size was of 128 points for chains of 10 and 12 atoms or 256 points for chains of 20 atoms.

## III. RESULTS AND DISCUSSION

In the present work a one-dimensional model system was examined in order to obtain a qualitative understanding of collision induced electronic excitation in a semiconductor substrate. The model system investigated consisted of a chain of atoms representing a one-dimensional crystal. This chain contained a single electron wave function whose properties, during the collision of a gas atom with the chain, were monitored. The chain atoms were assigned masses of silicon and the colliding projectile had the mass of xenon. The interaction potential between the chain atoms was assumed to be a LJ (12-6) potential where nearest neighbor and next nearest neighbor interactions were included. The LJ parameters used in the calculations were $\epsilon = 40\,240$ K (3.469 eV) and $\sigma = 1.782$ Å (3.367 bohr), while the assumed lattice constant was $a = 2.0$ Å. The interaction potential between the collider and the chain was taken to be a Morse function representing the coupling between the gas atom and the outermost chain atom. The parameters used in the calculation for this Morse function were: $D_e = 1006$ K (0.087 eV), $\beta = 1.5$ Å$^{-1}$ (0.794 bohr$^{-1}$) and $R_e = 2.5$ Å (4.72 bohr). The interaction of the electron with the solid (chain) was assumed to be given by a sum of pairwise screened Coulomb interactions between the electron and each one of the chain atoms [Eq. (2.7)]. In some of the simulations a direct interaction between the electron and the projectile was included. The functional form of this interaction is described in Eq. (3.1) and (3.2) below.

The initial condition of a given trajectory were obtained by using the following procedure:

(A) The electron wave function of the ground state, and the first two excited states, were calculated by the relaxation method.[17] This calculation was performed using a frozen chain in which all atoms were positioned at their lattice points. The calculation of the wave functions was converged up to nine digits.

(B) The electron was placed in its ground state and the integration of both quantum and classical equations of motion turned on. The integration was performed in a self-consistent manner until both subsystems (quantum and classical) relaxed to their equilibrium configurations. This equilibration procedure was performed in order to obtain the initial conditions for the trajectory. Typically about 2000–3000 time steps were needed for thermalization to take place.

(C) The gas atom was positioned at such a distance that the collider–chain interaction was practically zero. The projectile was assigned a predefined velocity directed towards the chain, and the trajectory integration was started.

(D) During the evolution of the trajectory, the electron's first three adiabatic states were evaluated (using the relaxation method[17]) after each 100 integration steps. Next, the current electronic wave function was projected onto these adiabatic states. The excitation probability was taken to be proportional to one minus the square of the overlap between the full wave function and the ground adiabatic state. The excitation to the first excited state was also evaluated, and usually carried most of the excitation amplitude.

(E) The trajectory was terminated after 50 000 integration steps (approximately 1.2 ps).

As described above, the initial electron wave function was calculated by using a static chain where the atoms were positioned at their lattice points. Since the chain was aimed to simulate a one-dimensional semiconductor, the energy difference between the ground and first excited states was defined as the band gap. The variation in the magnitude of this band gap could be achieved by either change of the chain length or by change of the nuclear charge on the chain atoms. In the present work the first possibility was chosen, namely, the value of the band gap was changed by the alternation of the chain length $N_c$. Three values of $N_c$ were investigated in this study, $N_c = 10$, 12, and 20. The corresponding band gap values were (for unit nuclear charge): 0.468, 0.346, and 0.163 eV, respectively.

The electron-chain potential together with the ground and first excited wave functions are shown in Fig. 1. These results correspond to a static chain. It should be noted that in addition to the $N_c$ movable chain atoms the last atom in the chain was coupled to two "wall" atoms which were fixed at their lattice points. The electron was allowed to interact with the $N_c$ chain atoms as well as the two wall atoms. Moreover, the last atom in the chain was also coupled to a fictitious particle whose motion was subject to a Langevin equation of motion. This fictitious particle was added to allow proper description of the energy dissipation from the chain to the bulk.[1(a),13] The electron was not coupled to this fictitious particle.

During the collision process between the gas atom and the chain, a large portion of the colliders translational energy was transferred to the chain. Due to the chosen mass combination in each scattering event there were two or more collisions between the projectile and the chain. The number of collisions during a trajectory was related to the initial kinetic energy of the projectile $E_0$. Hence, the amount of energy transfer also varied with $E_0$ and was found to be in the range 10%–50%. This energy transfer between the collider and

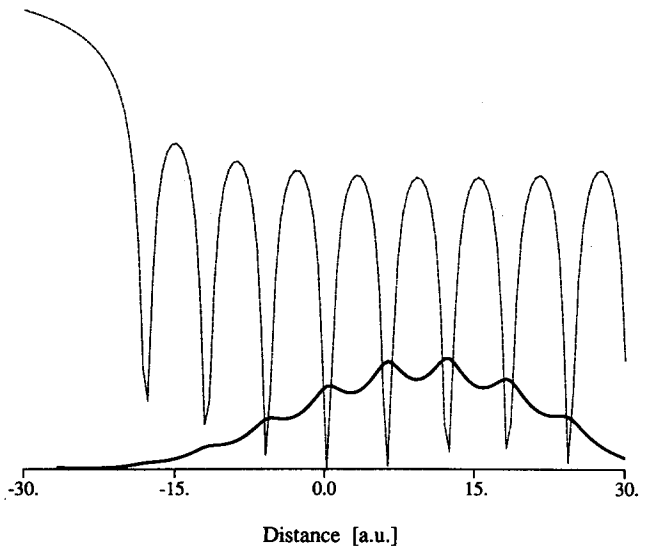


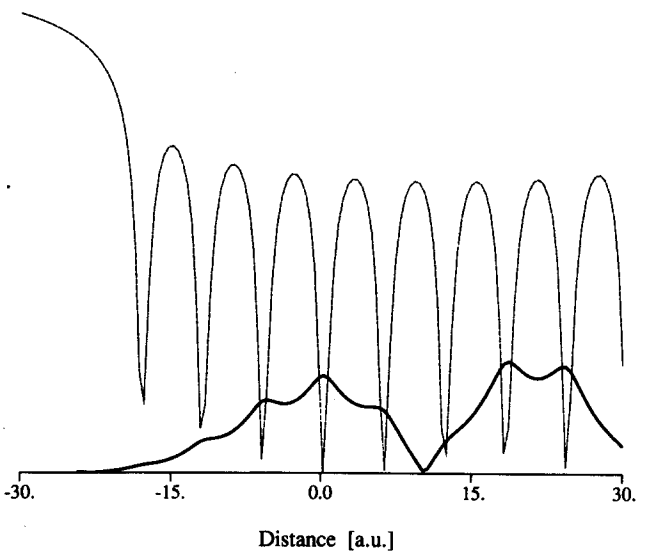


FIG. 1. The electronic wave function imbedded on the effective electron solid potential. (a) Shows the ground state and (b) the first excited electronic state for $N_c = 10$.

the chain caused an intensive phonon excitation (vibrations of the chain). Typical oscillations of the chain during a trajectory are shown in Fig. 2 for two values of $E_0$ and $N_c = 10$. Here the variation in chain length (distance between the first and last atoms) as a function of propagation time, are shown. It is clear that an increase in the value of $E_0$, results in a corresponding increase in the fluctuations of the chain length.

The goal of the present work was to establish a relationship between the excitation probability $P_e$ and various characteristics of the system. In particular, the influence of $E_0$, band gap magnitude, existence of impurities, and the direct interaction between the electron and the projectile on $P_e$ were investigated. The results obtained for each one of the

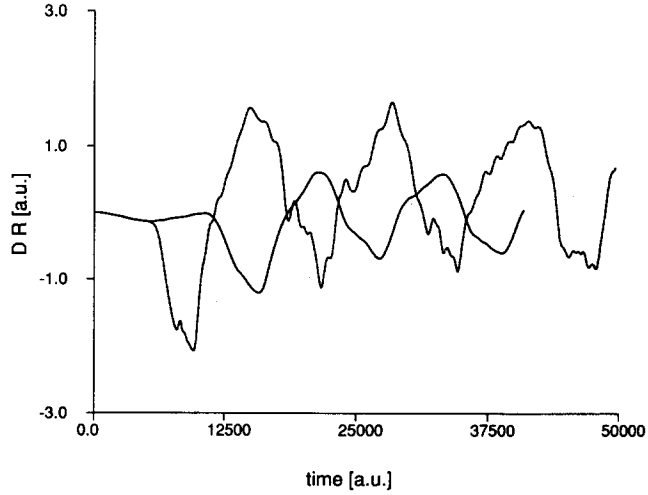


FIG. 2. Variation of chain length as a function of time for $E_0 = 30\,000$ K (solid line) and $E_0 = 130\,000$ K (dashed line) for $N_c = 10$ (2.59 and 11.21 eV, respectively).

above parameters will be described and discussed in the following subsections.

### A. Dependence on $E_0$ and band gap magnitude

The first system which was studied corresponds to $N_c = 10$. The form of the wave function at five instances during the a trajectory for $E_0 = 170\,000$ K (14.66 eV) is shown in Fig. 3. It is clear that in spite of the large magnitude of the chain's vibrations they induce only small variations in the shape of the wave function. The variation of electron energy, collider translational energy, and average chain ki-

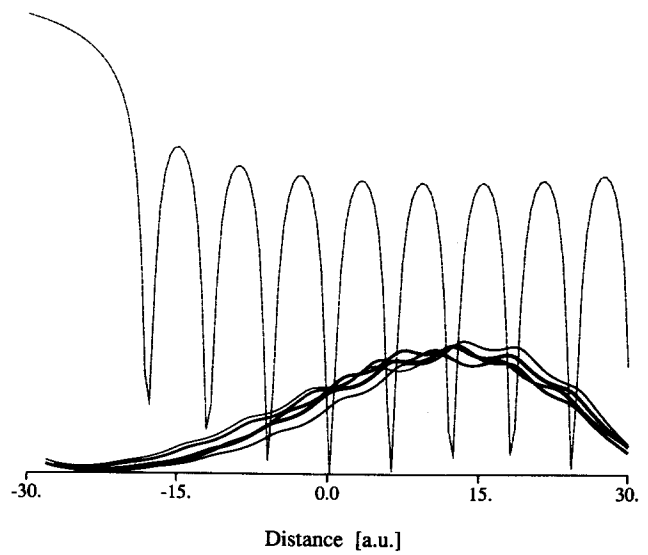


FIG. 3. The electronic wave function at five instances during the trajectory superimposed on the equilibrium electron chain potential. The various curves correspond to $t = 0$, 7000, 13 200, 20 000, 27 300 a.u.

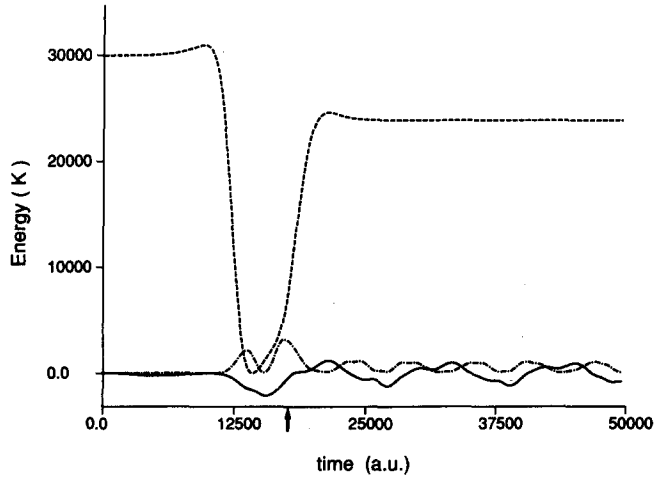


FIG. 4. Variation of electronic energy (solid line), gas atom energy (dashed line), and average chain kinetic energy (dashed–dot line) as a function of time for $N_c = 10$ and $E_0 = 30\,000$ K. The arrow indicates the instant of the second collision.

netic energy as a function of time are shown in Fig. 4 for $E_0 = 30\,000$ K (2.59 eV). At this value of $E_0$, about 25% of the projectile translational energy is transferred to the chain during two consecutive collisions. The fact that two consecutive collisions take place is evident from the change in the projectile's kinetic energy at $t = 16\,500$ a.u. (indicated by a small arrow). The energy transferred to the one-dimensional solid seems to be evenly distributed between the electron and the chain atoms. In both subsystems (electron and chain atoms) one can observe the existence of dumped oscillations in the energy values. The dumping is related to the energy dissipation to the rest of the solid which take place via the fictitious particle.

The magnitude of the electronic excitation probability during the evolution of a trajectory for $N_c = 10$ and two values of $E_0$, is shown in Fig. 5. Similarly, Fig. 6 presents the variation of $P_e$ for $N_c = 20$ and two values of $E_0$. Inspection of these results shows that in both cases the initial value of $P_e$ has a magnitude of approximately $10^{-10}$. This low value corresponds to the occupation of the excited state at room temperature (in all the calculations the surface temperature was taken to be 300 K). Inspection of these results shows that rapid oscillations in the magnitude of the excitation probability occur during the whole period of the trajectory propagation. These rapid oscillations correspond to transitions between the two states of the dynamical system under investigation.[19] The oscillations should be proportional to the energy difference between the two states, namely, the band gap in the example used. A short time averaging procedure was then used to filter out the high frequency component. Results of such a time averaged trajectory were practically identical to an average of over 15 trajectories chosen with the random initial vibrational phase of the chain.

Since a one-dimensional system has was in this work, the only feature with a random nature was the vibrational phase of the chain. Thus, the results should be averaged over this phase. As a result, most of the data described below corresponds to the outcome of a single trajectory which was time averaged.

Once the collision process starts, a large increase in excitation probability is observed. It is clear that the magnitude of this increase in $P_e$ strongly depends on the translational energy of the projectile and on the magnitude of the band gap (chain length). Even for the low collision energy, 50 000 K (4.31 eV), one obtains 3–4 orders of magnitude increase in the excitation probability. Inspection of Fig. 5 shows that even at large collision energies, when the amount of energy transferred to the solid is much larger than the magnitude of the band gap, only a small probability of excitation was obtained. This means that the energy channeled into the electronic degrees of freedom in the system, results in an adiabatic increase of the electron energy. In other words, the electron follows the nuclear motion adiabatically without

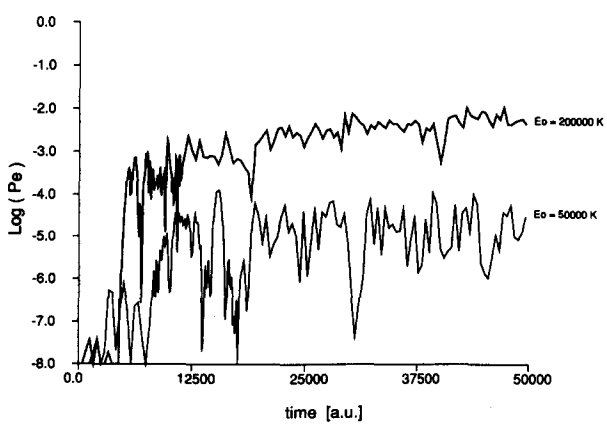


FIG. 5. The variation of the electronic excitation $P_e$ as a function of time for two values of $E_0$, 50 000 and 200 000 K, and $N_c = 10$ (4.31 and 17.24 eV, respectively).

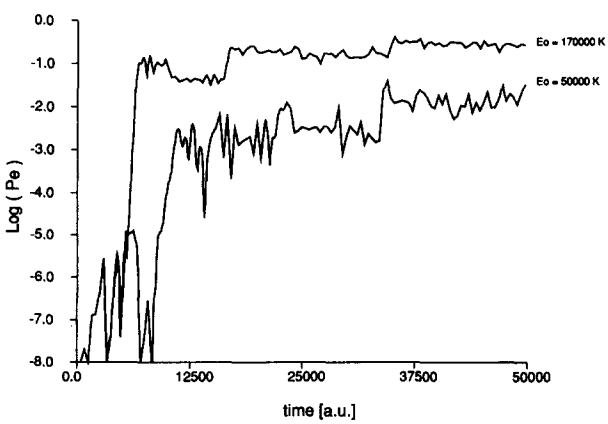


FIG. 6. Same as Fig. 5 for $E_0 = 50\,000$ and 170 000 K and $N_c = 20$ (4.31 and 14.66 eV, respectivly).

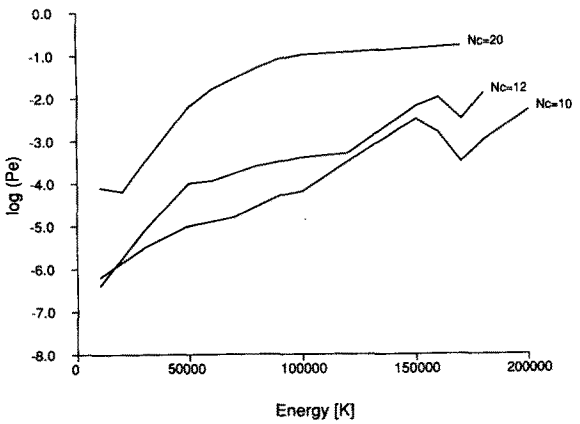


FIG. 7. The logarithm of the average electronic excitation as a function of the incident kinetic energy for three values of $N_c$, 10, 12, and 20.

exhibiting a large electronic excitation. On the other hand, it is clear from Figs. 5 and 6 that compared to the initial excitation probability (before the collision) there are many orders of magnitude increase in $P_e$ during and after the collision. Moreover, it is clear from these results that the amount of electronic excitation shows a marked increase when the band gap decreases.

In Fig. 7 the variation of the average value of $\log(P_e)$ as a function of the collider translational energy is shown for three values of the band gap (e.g., for $N_c = 10$, 12, and 20). Inspection of these results shows that for a given value of the band gap the excitation probability increases approximately exponentially with increasing values of $E_0$. For $N_c = 20$ (the smallest band gap) a saturation in the excitation above $E_0 = 100\,000$ K (8.62 eV) is obtained. At low $E_0$ values, there is a threshold value below which very little excitation occurred. This threshold value is classically equal to the band gap, however, due to the tunneling small amounts of electronic excitation occur even at smaller $E_0$ values. It is clear from the results in Fig. 7, that a decrease in the band gap value from 0.468 eV ($N_c = 10$) to 0.346 eV ($N_c = 12$) results in a relatively small increase in the excitation probability. This increase in $P_e$ is not monotonic, in the energy range of $E_0 = 50\,000$–$100\,000$ K (4.31–8.62 eV), where about one order of magnitude change is observed. For collision energies outside this range, the influence of the band gap magnitude on $P_e$ is less pronounced. Further decrease of the band gap to a value 0.163 eV ($N_c = 20$) shows an marked increase in the excitation probability. Here, one obtains a 2–4 orders of magnitude increase in the values of $P_e$ for any given $E_0$ value in the range studied. Thus, it seems that there is a stronger dependence of $P_e$ on the magnitude of the band gap, as compared to the dependence on the magnitude of the collision energy.

At high collision energies, $E_0 = 170\,000$ K (14.66 eV), a resonance behavior is observed for $N_c = 10$ and 12, while for $N_c = 20$ this energy corresponds to the saturation value of $P_e$. It has been verified that this resonance is real by calculating a few trajectories for each $E_0$ value around $E_0 = 170\,000$ K (and $N_c = 10$). The nature of the resonance is unclear at present and it is a subject for further investigation.

### B. Direct interaction between the electron and the projectile

In the past, Kirson *et al.* have calculated the energy transfer to an electron in the metal during the collision of various projectiles with the metal.[9] In these studies the energy transfer to the electron was due to the direct interaction between the electron and the collider. The functional form of the interaction was taken to be given by[9(b)]

$$V_{eg}(R_g - r_e) = -A_0 e^{-\mu(R_g - r_e)^2}, \tag{3.1}$$

where $A_0$ and $\mu$ were taken to be 0.25 a.u. and 0.17 bohr$^{-2}$, respectively. This form of the electron–projectile interaction potential accurately describes the results of electron scattering from atoms. In the work of Kirson *et al.*, only the attractive part of the potential was used, Eq. (3.1), since its range covered all the important range of electron–collider distances.

The present work was aimed to establish the relationship between the magnitude of electronic excitation in a semiconductor and the form of the direct electron–projectile potential (in addition to the electron–phonon interaction). However, in the energy range used in the present study the classical turning point of the collider was quite close to the surface, hence it seemed therefore that to the potential in Eq. (3.1) a repulsive part should be added. Thus, the form used here to represent $V_{eg}$ was

$$V_{eg}(R_g - r_e) = -A_0 e^{-\mu(R_g - r_e)^2} + B_0 e^{-\alpha(R_g - r_e)^2}, \tag{3.2}$$

where the values of the four parameters in Eq. (3.2) are given in Table I.

The results of four typical trajectories are shown in Fig. 8. These results describe the variation of the electronic excitation probability during the evolution of the trajectory for $E_0 = 150\,000$ K (12.93 eV) and $N_c = 10$. Curve 1 (in Fig. 8) corresponds to an attractive electron–projectile interaction without a repulsive part, curves 2 and 3 correspond to a sum of attractive and repulsive terms (with parameters described in Table I), while curve 4 includes only electron–phonon interaction and was added as reference. It is clear from these results that when the electron–projectile interaction contains only an attractive part, a huge increase in the magnitude of $P_e$ is obtained. The magnitude of the excitation probability reaches a saturation value close to unity during the approach of the projectile to the chain. This situation, with only an attractive electron–collider interaction, may lead to the ionization of the projectile where an electron is transferred from the solid to the gas atom. Indeed, inspection of the electron wave function during the approach of the projectile, shows that it starts to localize around the position of the gas atom when it is located near the classical turning point. However, the grid used to span the electron wave function was not large enough to allow charge transfer from the chain to the collider.

TABLE I. Parameters of potential, grid, and propagation method, used in the simulation of electon–hole pair dynamics.

| Electron solid potential | Electron collider potential | | | |
|---|---|---|---|---|
| $V_{ei}=\frac{Z_i}{[(r_e-r_i)^2+\alpha^2]^{1/2}}$ | $V_{eg}=-A_0e^{-\mu(R_g-r_e^2)}+B_0e^{-\alpha(R_g-r_e)^2}$ | | | |
| $Z_i=0.1$ a.u. | $A_0=$ | 0.25 | 0.75 | 1.5 |
| $\alpha=0.1$ a.u. | $\mu=0.17$ a.u. | | | |
| $\Delta r=3.779\,504$ a.u. | $B_0=$ | 0.3824 | 1.1472 | 1.6944 |
| | $\alpha=0.34$ a.u. | | | |
| Masses | $m_{Si}=28.12$ amu | | | |
| | $m_{Xe}=131.29$ amu | | | |
| Grid | | | | |
| for 10 atoms | $N=128$ | $\Delta x=0.295\,274$ | | |
| for 12 atoms | $N=128$ | $\Delta x=0.354\,329$ | | |
| for 20 atoms | $N=256$ | $\Delta x=0.295\,274$ | | |
| Chebyshev time propagation | | | | |
| convergence criteria | | $\epsilon<10^{-9}$ | | |
| time step for relaxation | | $\Delta t=4.133\,5$ a.u. | | |
| time step for propagation | | $\Delta t=4.133\,50$ a.u. | | |
| total number of steps | | $N_t=12\,000$ | | |

When a repulsive part was added to $V_{eg}$ all the additional electronic excitation was suppressed. Comparison between the results of curves 2, 3, and 4 shows that there is practically no difference between these trajectories. Thus, if only the attractive part of the potential between the electron and the projectile is included, $V_{eg}$ dominates the electronic excitation mechanism. However, if a repulsive part is added to $V_{eg}$, the dominant process which lead to electronic excitation is the electron–phonon coupling.

### C. The influence of impurities

It is well known that real semiconductor crystals exhibit some amount of defects. These defects may be vacancies, interstitial atoms, and various impurities. In some situations these defects tend to segregate to the surface, hence, their concentration at the solid surface may be quite large. Moreover, in many cases the semiconductor is doped by a given impurity (to alter its electronic properties) where the dopant concentration and distribution in the solid is well defined. In the following calculations will be described in which the existence of vacancies and impurities were examined.

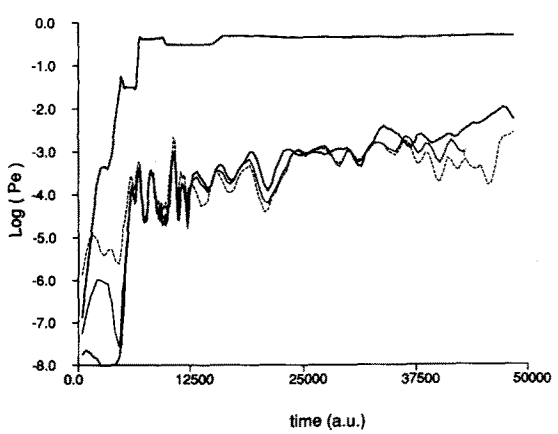


FIG. 8. Electronic excitation as a function of time for $N_c=10$ and $E_0=150\,000$ K (solid line). Curve 1 corresponds to an attractive only gas atom electron interaction, the two light dashed lines include a repulsive term in the electron gas atom interaction potential, Eq. (3.2), and the dark dashed line is a reference without any electron gas interaction.

The simplest way to simulate the existence of an impurity in the system described above was to alter the magnitude of the nuclear charge $Z_i$ on a given atom in the chain. If the nuclear charge on one of the chain atoms was taken to be zero, the electron did not interact with this atom. Such a situation corresponds to the existence of a vacancy (from the electrons point of view). To simulate the existence of an impurity atom, $Z_i$ was varied between the values zero and two. The electron–chain potential and the ground state wave function of the electron for three values of $Z_5$ (for a static chain of length $N_c=10$) are shown in Figs. 9. In Fig. 9(a), $Z_5=0.01$ corresponds to the existence of a vacancy in the middle of the chain. The existence of a vacancy is clearly seen in the form of the electron–chain interaction potential. In this case the electron is repelled from the vacancy and its wave function is clearly localized in the inner part of the chain. Similar behavior was obtained for $Z_5=0.5$ as shown in Fig. 9(b). Once $Z_5=1.5$, Fig. 9(c), a deep well is formed at the chain center and the electron wave function is highly localized at this well. In Fig. 10 the electron–chain interaction potential at $t=0$ ($Z_5=0.5$ and $N_c=10$) is shown together with the electronic wave function at a number of time intervals during the collision process. It is clear that once the collision starts, the chain compresses. As a result, the amplitude of the wave function near the surface increases. Moreover, it is clear that the variations in the electronic wave function mimic the motion of the chain atoms.

The variation of the excitation probability during the

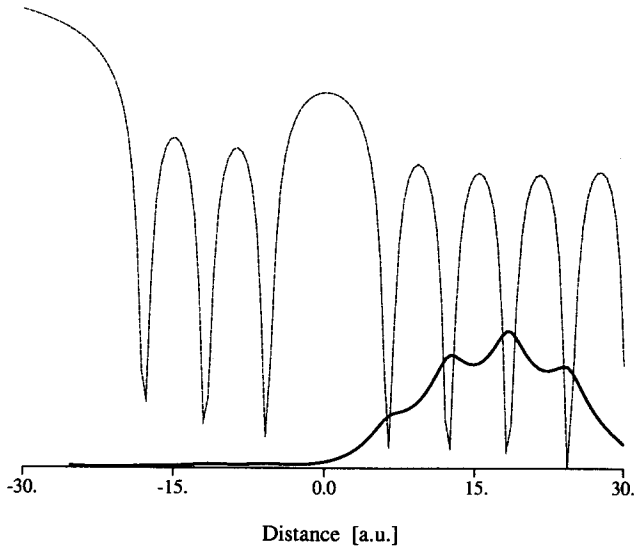


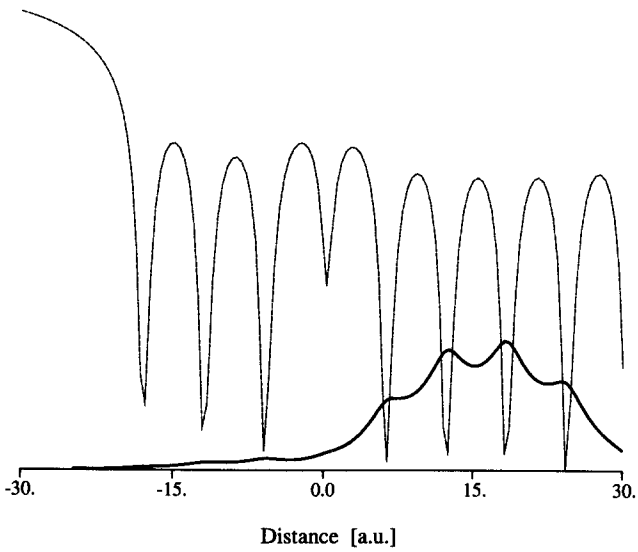


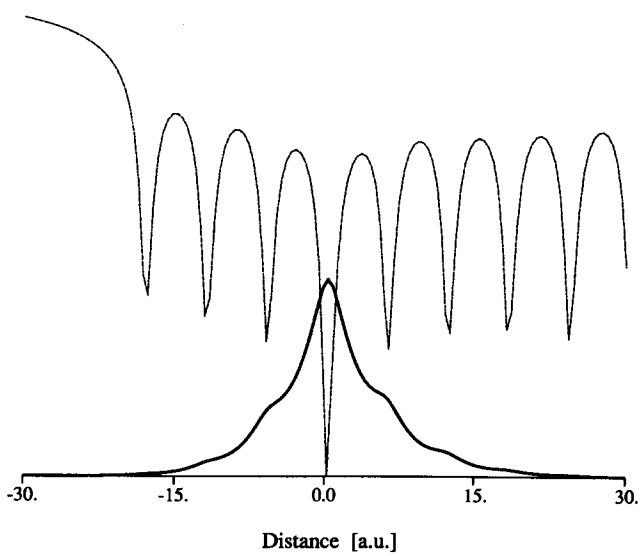


FIG. 9. The ground electronic wave function imbedded on the potential for three values of $Z_5$ and $N_c = 10$. In (a) $Z_5 = 0.01$. In (b) $Z_5 = 0.5$, and in (c) $Z_5 = 1.5$.

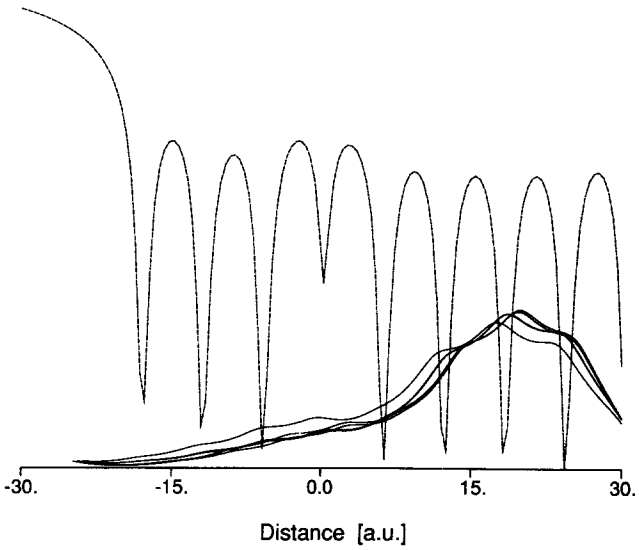


FIG. 10. The electronic wave function at five instances superimposed on the equilibrium electron chain potential for $Z_5 = 0.5$ and $E_0 = 170\,000$ K and $N_c = 10$. The various curves correspond to $t = 0$, 5000, 9000, 11 000, 13 000 a.u.

evolution of the trajectory for five values of $Z_5$ ($N_c = 10$ and $E_0 = 170\,000$ K) are shown in Fig. 11. Curve 5 in Fig. 11 corresponds to $Z_5 = 1.0$, namely, a perfect chain without impurity. Curve 1 corresponds to $Z_5 = 0.01$ which represents the existence of a vacancy, while, curves 2, 3, and 4 correspond to $Z_5 = 0.5$, 0.75, and 0.25, respectively. It is clear that the existence of any type of defect in the chain (vacancy or impurity) results in a marked increase of the excitation probability. The largest values of $P_e$ were observed for $Z_5 = 0.5$ which were about two orders of magni-

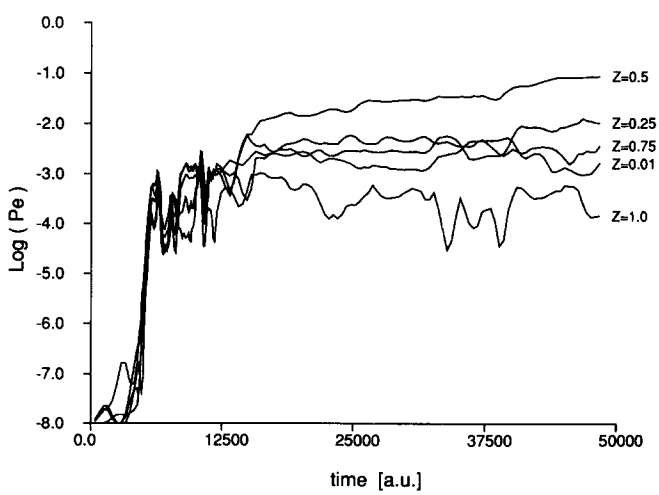


FIG. 11. The variation of the electronic excitation $P_e$ as a function of time for $E_0 = 170\,000$ K and $N_c = 10$, for five values of $Z_5$, 0.01, 0.25, 0.5, 0.75, and 1.0

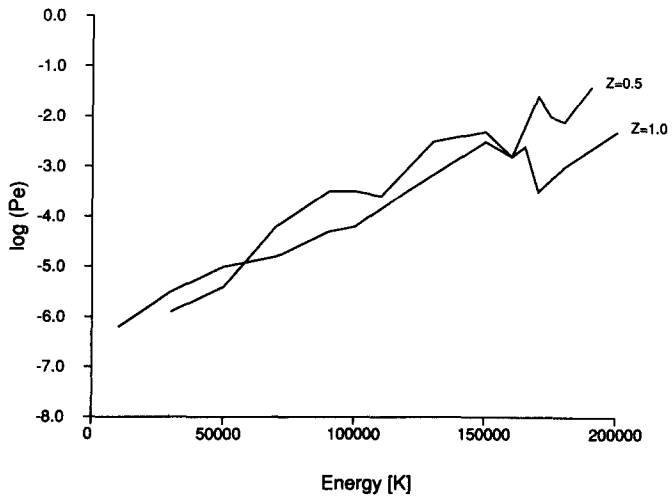


FIG. 12. The logarithm of the average electronic excitation as a function of the incident kinetic energy for two values of $Z_5$, 0.5 and 1.

tude larger than those obtained for a perfect chain (curve 5). For other values of $Z_5$ (curves 2, 3, and 4) one obtains an increase in the magnitude of $P_e$ (as compared to $Z_5 = 1.0$) but not as extensive a one as the one observed for $Z_5 = 0.5$. This behavior is not uniform in the whole range of $E_0$ studied here. In Fig. 12 the variation of $\log(P_e)$ as a function of $E_0$ is shown for $Z_5 = 0.5$ and 1.0. Except for $E_0$ values below 50 000 K the magnitude of $P_e$ for $Z_5 = 0.5$ is larger that those for $Z_5 = 1.0$ by about one order of magnitude. At low incidence energies the situation is reversed. The large difference in $P_e$ at $E_0 = 170\,000$ K is related to the resonance which occurs for $Z_5 = 1.0$ at this energy. It was not found for $Z_5 = 0.5$ (see Fig. 12).

## IV. SUMMARY

The collision induced electron–hole pair formation in a semiconductor has been examined using a single electron and one-dimensional solid model calculations. The goal of the study was to investigate the relationship between the electronic excitation probability and the various characteristics of the solid. It was found that even at low collision energies, a large probability for electronic excitation occurs (relative to the thermal value of $P_e$). The magnitude of the excitation probability was found to markedly increase when the collision energy was increased. A strong dependence of $P_e$ on the magnitude of the band gap was found. This dependence tended to be equivalent to the dependence on $E_0$. In addition, the existence of defects and impurities in the solid were shown to result in an additional increase in the value of $P_e$. The dependence of $P_e$ on the direct electron–projectile interaction was also examined. It was found that this interaction was the dominant one if only attractive interactions are considered. On the other hand, it was unimportant (compared to the electron–phonon interaction) when both attractive and repulsive electron–projectile interactions were used. As a conclusion ionization or electron attachment to the colliding projectile is an important contribution to the excitation probability if this channel is available.

A comparison of the results of these calculations with the experimentally observed values of $P_e$[9] shows that the experimental values are about one order of magnitude larger than those obtained here. However, if one takes into account that the real surface exhibits large number of defect sites and impurity atoms which may contribute to electronic excitation the discrepancy between the experimental and the calculated results is diminished. In addition, in a three-dimensional case collision of energetic atoms with the surface may cause sputtering of surface atoms. This process may contribute to the increase of $P_e$.

In the future, the plan is to generalize the model used here to include electron–electron interactions and a two-dimensional solid model. Thus, sputtering processes will be allowed and their contribution to the electronic excitation will be examined.

## ACKNOWLEDGMENTS

This research was supported by a grant from the Binational United States–Israel Foundation for Scientific Research. The Fritz Haber Research Center for Molecular Dynamics is supported by the Minerva Gesellschaft für die Forschung, GmbH München, Federal Republic of Germany.

[1] (a) Y. Zeiri, J. J. Low, and W. A. Goddard, J. Chem. Phys. **84**, 2408 (1986); (b) Y. Zeiri, Surf. Sci. (to be published).
[2] J. D. Beckerle, A. D. Johnson, and S. T. Ceyer, Phys. Rev. Lett. **62**, 685 (1989).
[3] See for example: (a) E. Kolodney and A. Amirav, J. Chem. Phys. **79**, 4648 (1983); (b) R. B. Gerber and R. Elber, Chem. Phys. Lett. **107** 141 (1984); (c) R. B. Gerber and A. Amirav, J. Phys. Chem. **90**, 4483 (1986); (d) A. Amirav, M. J. Cardillo, P. L. Trevor, C. Lin, and J. C. Tully, J. Chem. Phys. **87**, 1796 (1987); (e) A. Danon, E. Kolodney, and A. Amirav, Surf. Sci. **193**, 132 (1988).
[4] M. S. Connolly, E. F. Green, C. Gupta, P. Marzuk, T. H. Morton, C. Parks, and G. Staker, J. Phys. Chem. **85**, 235 (1981).
[5] J. F. de la Mora, J. Chem. Phys. **82**, 3453 (1985).
[6] (a) S. L. Tang, J. D. Beckerle, M. B. Lee, and S. T. Ceyer, J. Chem. Phys. **84**, 6488 (1986); **85**, 1693 (1986); (b) J. D. Beckerle, A. D. Johnson, Q. Y. Yang, and S. D. Ceyer, J. Chem. Phys. **91**, 5756 (1989).
[7] T. P. Beebe Jr., D. W. Goodman, B. D. Kay, and J. T. Yates, J. Chem. Phys. **87**, 2305 (1987).
[8] A. Dannon, E. Kolodney, and A. Amirav, Surf. Sci. **193**, 132 (1988).
[9] (a) Z. Kirson, R. B. Gerber, and A. Nitzan, Surf. Sci. **124**, 279 (1983); (b) Z. Kirson, R. B. Gerber, A. Nitzan, and M. A. Ratner, *ibid.* **137**, 527 (1984).
[10] (a) J. W. Gadzuk and H. Metiu, Phys. Rev. B **22**, 2603 (1980); (b) H. Metiu and J. W. Gadzuk, J. Chem. Phys. **74** 2641 (1981).
[11] K. Schonhammer and O. Gunnarsson, Phys. Rev. B **22**, 1629 (1980).
[12] A. Amirav and M. J. Cardillo, Phys. Rev. Lett. **57**, 2299 (1986); P. S. Weiss, P. L. Trevor, K. Kern, A. Vom Felde, and M. J. Cardillo, Surf. Sci. **226**, 191 (1990).
[13] See for example: (a) B. J. Garrison and S. A. Adelman, Surf. Sci. **66**, 253 (1977); (b) J. C. Tully, J. Chem. Phys. **73**, 1975 (1980); (c) R. R. Lucchese and J. C. Tully, Surf. Sci. **137**, 570 (1983).
[14] A. Selloni, P. Carnevali, R. Car, and M. Parrinello, Phys. Rev. Lett. **59**, 823 (1987).
[15] R. N. Barnett, U. Landman, G. Rajagopal, and A. Nitzan, Isr. J. Chem. **30**, 85 (1990), and references therein.

[16] J. Schnitker and R. J. Rosski, J. Chem. Phys. **86**, 3462 (1987).
[17] R. Kosloff and H. Tal-Ezer, Chem. Phys. Lett. **127**, 223 (1986).
[18] R. Kosloff, J. Phys. Chem. **92**, 2087 (1988); C. Leforestier, R. Bisseling, C. Cerjan, M. Feit, R. Friesner, A. Guldberg, A Hammerich, G. Julicard, W. Karrlein, H. D. Meyer, N. Lipkin, O. Roncero, and R. Kosloff, J. Comput. Phys. (to be published).
[19] See for example: C. Cohen-Tannoudji, B. Diu, and F. Laloe, *Quantum Mechanics* (Wiley, France, 1977) p. 413.